

Article

Research on the Power Output Characteristics of a Coupling Transformer in D-FACTS

Zhimin He ¹, Shuo Zhang ², Yadong Liu ³, Fan Wu ^{3,*} , Gehao Sheng ³ and Xiuchen Jiang ³

¹ Engineering Training Center, Shanghai University of Engineering Science, Shanghai 201620, China; rosahzmin@hotmail.com

² State Grid Jibei Electric Power Research Institute, Beijing 100045, China; zhshdwill@163.com

³ School of Electronic Information and Electrical Engineering, Shanghai Jiao Tong University, Shanghai 200240, China; lyd@sjtu.edu.cn (Y.L.); shenghe@sjtu.edu.cn (G.S.); xcjiang@sjtu.edu.cn (X.J.)

* Correspondence: yzwufan@sjtu.edu.cn

Received: 11 October 2019; Accepted: 8 December 2019; Published: 10 December 2019



Abstract: The series coupling distributed flexible AC transmission system (D-FACTS) device couples the secondary side compensating reactance to the primary side based on the principle of transformer, thus realizing the goal of adjusting the transmission line parameters and controlling the distribution network flow. The coupling transformer is the most important power conversion part in the D-FACTS device but has different working principles of mutual inductor. The magnetizing current of the coupling transformer changes within a large range, which makes the traditional power output model of mutual inductor inapplicable. In this paper, the power output model of coupling transformer was constructed by viewing the coupling transformer as a constant current source. Moreover, the corresponding relationship between the output power of the transformer and related parameters, as well as between variations of reactive output power and active loss power with load changes, was analyzed. Some conclusions were drawn: (1) the output power characteristic curve of the coupling transformer was acquired; (2) given a constant line current, the maximum power was achieved when the system's capacitive reactance and the internal resistance of the transformer matched, and the maximum power was unrelated to the number of turns of the coupling transformer; (3) the output power changed with the variation of the line current, and there was a proportional relationship between the maximum power and the square of the line current. Next, the relationship between the maximum output power and the air gap thickness of the magnetic core was discussed. Finally, these conclusions were proved accurate via experiments.

Keywords: D-FACTS; power output characteristics; coupling transformer

1. Introduction

The flexible AC transmission system (FACTS) introduces the technique of modern power electronics, a microelectronic technique, communication technology, and control technology into the AC transmission system [1]. It can adjust the impedance, voltage, phase, and power of the AC transmission system flexibly and quickly, thus realizing the goals of improving the delivery capacity of the transmission lines, damping system oscillation, and improving system stability, power quality, and reliability [2,3]. The development of a smart grid puts forward increasingly high requirements on the miniaturization and low cost of FACTS. Thus, the new distributed FACTS (D-FACTS) was proposed [4–7]. D-FACTS is composed of multiple distributed FACTS devices on the transmission lines. Each FACTS device provides certain compensation, and different devices make flexible responses through communication commands to enable a fast collaborative adjustment of the transmission line parameters. Various D-FACTS devices have been applied successfully in the power transmission system.

According to the working principle, a FACTS device can be divided into the thyristor-controlled series compensation (TCSC), the static synchronous series compensator (SSSC), the unified power flow controller (UPFC), etc. The D-FACTS device distributes these devices into transmission lines to control the line power flow. To meet the requirements on miniaturization and low cost, the D-FACTS device hangs on the transmission line and mainly applies a series coupling circuit design. Commonly distributed series coupling FACTS controllers in engineering include the distributed series reactance (DSR), the distributed series capacitor (DSC), the distributed static series compensator (DSSC) [7–9], etc.

To realize the series coupling structure, the coupling transformer becomes an important component of D-FACTS. The magnetic core of the coupling transformer has an open structure and can be hung on transmission lines, thus avoiding the insulation problem. Transmission lines can be viewed as the single-turn primary winding of the coupling transformer, and the compensating circuit is connected at the secondary side of the coupling transformer, which is quickly controlled through a composite switch or inverter, realizing power conversion. Such design is applicable to local control, fast and flexible, easy to install, and can be used repeatedly on different transmission lines.

Because the D-FACTS device is hung on transmission lines, the operating environment and conditions will influence the design indicators of the device. Each independent D-FACTS device must be able to provide certain compensations to achieve the overall functions, but the safe codes of the transmission lines put forward strict requirements with regard to the weight and size of the device on the transmission lines. Therefore, the D-FACTS device needs a high unit power density in order to provide adequate compensation power while meeting the design standards. Unlike traditional power converters, the D-FACTS device is installed outdoors. Because natural wind cooling is the only means of heat dissipation, the active loss of the device must be as small as possible to protect the reliability of the D-FACTS device. The coupling transformer is the main power conversion part and the heaviest part in the D-FACTS device. The coupling transformer design will determine the unit power density and the heat dissipation of the D-FACTS device directly.

Most of the existing research on D-FACTS devices focuses on operating characteristics and control strategies [6,10–13]. Few researchers have studied the performance and structural characteristics of the key device—the coupling transformer. The unique working mode of the coupling transformer also determines its uniqueness among conventional transformers. The magnetizing current of the coupling transformer will change within a large range. The magnetic core of the coupling transformer has to work in the linear region for the purpose of compensation, which makes the power output model of the traditional mutual inductor inapplicable. As a result, it is very necessary to further explore the power output characteristics [14] of the coupling transformer in the D-FACTS device.

Based on the working characteristics of the D-FACTS device, the input of the coupling transformer was viewed as a constant flow source, and the power output model of the coupling transformer is constructed in this paper. The relationships between the reactive output power of the coupling transformer, the load size, and the number of turns at the secondary side and line currents are analyzed. The inductive and capacitive power compensations are discussed, and the load corresponding to the maximum power are deduced. Variations of reactive output power and active loss power with load are compared, and suggestions concerning power density and heat dissipation, as well as the optimization of the D-FACTS device, are given. Finally, the influence of the air gap changes of the magnetic core on the output power are deduced and verified. The above conclusions were proven accurate by the experiments. Studying the power output characteristics of the coupling transformer in D-FACTS devices can provide guidance for the design and optimization of these devices so that the D-FACTS device will have more comprehensive functions, a simpler structure, and a lower cost. The optimized D-FACTS device can control the distribution network flow more effectively and increase the intelligence of the power system [15,16].

2. Power Output Characteristics

The basic structure of the series coupling D-FACTS device can be described by a mini series compensator: the D-FACTS device couples the series reactance into the primary side through the coupling transformer and changes the coupled reactance of the primary side by changing the reactance of the secondary side. The overall structure is shown in Figure 1. The secondary side consists mainly of a short-circuit switch (S_m), capacitive reactance (X_{cf}), induction reactance (X_{lf}), switches (S_1 and S_2), control module, power supply module, and communication module. The short-circuit switch (S_m) controls the operating status of the compensator. When it is closed, the compensator exits from the operation. The power supply module harvests electricity directly from the transmission lines and provides energy supports to the whole system. The control module controls S_1 and S_2 according to a certain law to achieve a flexible adjustment of the compensating reactance. The communication module is mainly for interaction with the backstage supporter.

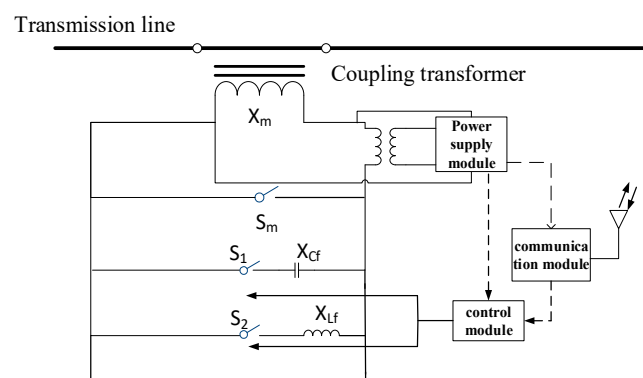


Figure 1. Structure of the compensation device.

The fundamental magnetization curve of the magnetic core materials in the coupling transformer is shown in Figure 2. The working points of the traditional current transformer and the power transformer change within a small range. For example, the current transformer works at the point close to (a), and the power transformer works at the point close to (c). The coupling transformer of the D-FACTS device must work in the linear region (b) to realize the compensation function. The working point changes with the secondary side load, which will change the corresponding output voltage and output current accordingly.

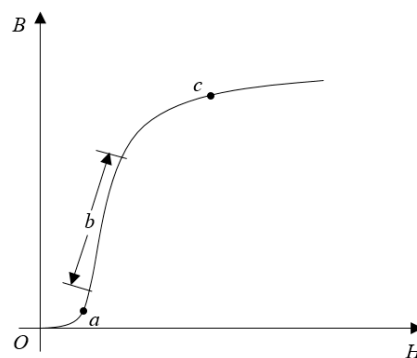


Figure 2. The fundamental magnetization curve of magnetic core materials.

Suppose that the current passing through the transmission line is I_1 ; the inner diameter, outer diameter, thickness, and number of turns of the coupling transformer are D_i , D_o , h , and N_2 , respectively.

If the coupling transformer works in the linear region, the induced voltage (e_2) of the secondary side of the transformer is [17].

$$e_2(t) = N_2 \frac{\mu h}{2\pi} \ln \frac{D_o}{D_i} \frac{di_\mu}{dt} \tag{1}$$

where μ is the effective magnetic permeability of the magnetic core and i_μ is the magnetizing current.

According to the equilibrium equation of the magnetomotive force:

$$\dot{I}_1 N_1 + \dot{I}_2 N_2 = \dot{I}_m N_1 \tag{2}$$

where N_1 is the number of turns of the primary coil ($N_1 = 1$ in this paper), N_2 is the number of turns of the secondary coil, and \dot{I}_m is the exciting current.

Considering the magnetic hysteresis loss, \dot{I}_m could be decomposed into the current parallel to the magnetic flow (\dot{I}_μ) and the magnetic hysteresis loss current perpendicular to the magnetic flow (\dot{I}_{Fe}). Thus, the following is true.

$$\dot{I}_\mu + \dot{I}_{Fe} = \dot{I}_m \tag{3}$$

The iron loss of the magnetic core can be calculated according to Steinmetz's empirical formula:

$$P_v = C_m f^\gamma B^\beta \tag{4}$$

where P_v is the loss per unit volume in mW per cubic centimeter, f is the working frequency in kilohertz, B is the amplitude of magnetic flux density, and C_m , γ , and β are empirical parameters.

The hysteresis resistance of the magnetic core is approximately viewed as R_m ; then,

$$P_v = R_m \dot{I}_{Fe}^2 \tag{5}$$

By comparing Equations (4) and (5), the iron loss current I_{Fe} could be expressed as follows:

$$I_{Fe} = C_1 I_\mu^k \tag{6}$$

Omitting leakage inductances and internal resistances of the primary and secondary sides, the loading model of the simplified coupling transformer is shown in Figure 3, based on the above analysis, where R_{Fe} is the iron loss resistance, X_L is the magnetic inductance, and Z is the load. Contrary to what happens in traditional transformers, the input voltage E_1 of the coupling transformer changes with the loads, while the input current I_1 is independent from the load. Therefore, it is more appropriate to view the coupling transformer as a constant flow source.

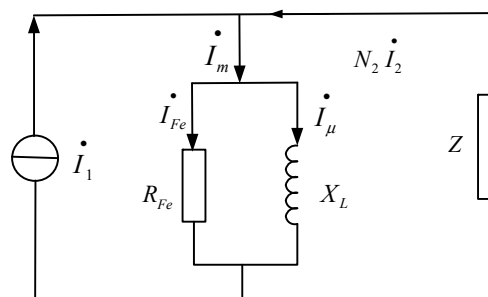


Figure 3. Simplified loading model of the coupling transformer.

Suppose the load (Z) of the compensation device is the pure capacitive circuit (X_C). The vector diagram (Figure 4) of the loading model of the coupling transformer can be drawn according to Figure 4.

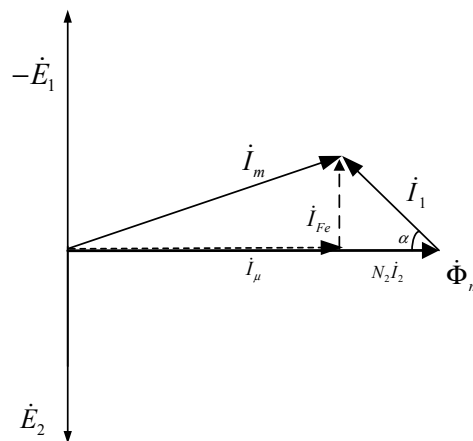


Figure 4. Vector diagram of the loading model of the coupling transformer.

According to Figure 4,

$$I_1 \sin \alpha = I_{Fe} \quad (7)$$

$$I_2 N_2 - I_1 \cos \alpha = I_{\mu} \quad (8)$$

The series compensator has to offer reactive compensation to the system. Therefore, the output powers mentioned in this paper all refer to the compensated reactive power Q . If the voltage compensated by the secondary side to the primary side is E_1 , and its included angle with I_1 is φ , then

$$e_1 = \frac{e_2}{N_2} = \frac{\mu h}{2\pi} \ln \frac{D_o}{D_i} \frac{di_{\mu}}{dt} \quad (9)$$

$$Q = E_1 I_1 \sin \varphi = \mu h f \ln \frac{D_o}{D_i} I_1 I_{\mu} \cos \alpha \quad (10)$$

Combining Equations (6), (7), and (10),

$$Q = \mu h f \ln \frac{D_o}{D_i} C_1^{-\frac{1}{k}} I_1^{1+\frac{1}{k}} (\sin \alpha)^{\frac{1}{k}} \cos \alpha \quad (11)$$

The maximum output power Q_{max} can be gained from the following equation:

$$\frac{dQ}{d\alpha} = \mu h f \ln \frac{D_o}{D_i} C_1^{-\frac{1}{k}} I_1^{1+\frac{1}{k}} \left(\frac{1}{k} (\sin \alpha)^{\frac{1}{k}-1} \cos^2 \alpha - (\sin \alpha)^{\frac{1}{k}+1} \right) = 0 \quad (12)$$

Given a fixed I_1 , the α_0 [18,19] that makes $Q = Q_{max}$ can be determined by choosing the appropriate load capacitance:

$$Q_{max} = I_1^{1+\frac{1}{k}} f(\alpha_0) \quad (13)$$

The deduction of the mathematical relationship between the angle α and the load capacitance C is shown in Appendix A.

It can be known from Equation (13) that when the coupling transformer works in the linear region, Q_{max} is related to C and I_1 but unrelated to the number of turns of the transformer (N_2). The empirical parameter k value is approximately 1. Therefore, Q_{max} is appropriately proportional to the square of I_1 . Given a fixed I_1 , Q changes with C . In this process, Q changes from negative to positive and presents the minimum, zero, and maximum values. Calculations of the minimum, maximum, and zero values of Q are shown in Appendix B.

The whole circuit can be viewed as changing from inductive to capacitive with the gradual increase of C . In this case, X_L and X_C are viewed as an integral reactance (X) that is capacitive and inductive. When C is very small, X is inductive. When the module of its inductive reactance is equal to

the impedance of iron loss resistance (R_{Fe}) (known as the matching between the system's inductive reactance and internal resistance), the negative maximum of Q is achieved. At this moment, the device compensates the inductive reactive power to the transmission lines. When X_C and X_L are mutually offset, $Q = 0$. When C is very large, X is capacitive. When the module of its capacitive reactance is equal to the impedance of iron loss resistance (R_{Fe}) (known as the matching between the system's capacitive reactance and internal resistance), the positive maximum of Q is achieved. At this moment, the device compensates the capacitive reactive power to the transmission lines.

After the magnetic core size is fixed, the unit power density of the coupling transformer is only related with the output power. Therefore, the variation of power density can be known from the power output characteristic curve of the coupling transformer. Additionally, the heat dissipation of the coupling transformer is attributed to the active loss on R_{Fe} . The active power (P) can be expressed by Equation (14), which also reflects the relationship between P and α . Therefore, heat dissipation can be controlled within the acceptable range by controlling the load capacitance.

$$P = \frac{E_2 I_{Fe}}{N_2} = \mu h f \ln \frac{D_o}{D_i} C_1^{-\frac{1}{k}} I_1^{1+\frac{1}{k}} (\sin \alpha)^{1+\frac{1}{k}} \quad (14)$$

When the line current, the magnetic core size, and the number of turns are fixed and when the load capacitance is changing, the relationship among the reactive output (Q), the active loss (P), and the load capacitance (C) can be deduced from Equations (11) and (14), which is shown in Figure 5.

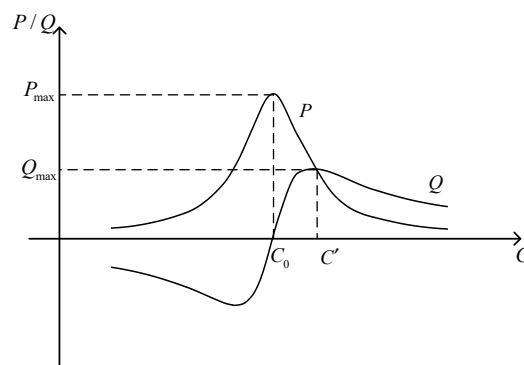


Figure 5. Relation curves among reactive output, active loss, and load capacitance.

Based on the above calculations, with the increase of C , Q decreases firstly to the negative maximum, quickly increases to positive, and then begins to decrease again after reaching the positive maximum; P increases firstly to the maximum and then decreases. It can be seen that when $Q = 0$, P reaches the peak; when Q is at the maximum, P is equal to Q in numerical value.

3. Experimental Test

A cold rolling silicon steel sheet 30Q110 was used as the experimental magnetic core to verify the above conclusions under different experimental conditions. Basic parameters of the magnetic core are listed in Table 1.

Table 1. Parameters of the magnetic core.

Parameters	Numerical Value
Inner diameter D_i	55 mm
Outer diameter D_o	75 mm
Thickness h	30 mm
Density	7.35 g/cm ³
C_1	0.22
k	0.95

3.1. Power Output Characteristic Curve

An experiment was designed to verify the power output characteristics of the coupling transformer (Figure 6). In the experiment, a three-phase power source with model CL303 and a digital oscilloscope with 10 GSa/s were used. In Figure 6, the power source generates a constant current to simulate the load current on the transmission lines. The ratio of the current transformer (CT) is 200 A/333 mA, and the oscilloscope records the voltage waveform on the resistor connected to the CT, which expresses the primary side current. The load capacitor was connected to the output end of the coupling transformer through a series connection. The secondary side output voltage (U) under different load capacitances (C) was recorded and converted into the primary side. Meanwhile, the amplitude of the output current (I) of the power source, as well as the phase difference (φ), were recorded. Finally, the inactive output of the coupling transformer was calculated: $Q = \frac{UI \sin \varphi}{N}$.

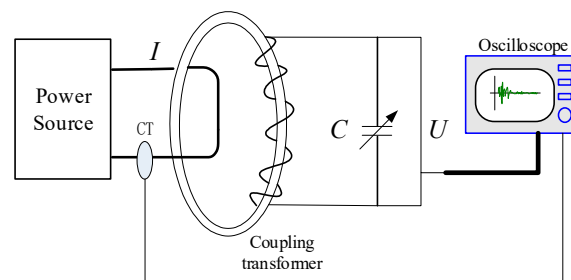


Figure 6. Experiment with the power output characteristics of the coupling transformer.

Typical experimental waveforms are shown in Figure 7. Ch1 is the voltage waveform on load capacitance, and Ch2 is the voltage waveform on the resistor connected to the CT. The phase difference between Ch1 and Ch2 is the phase difference between input and output. And Figure 8 shows the test site of the experiment.

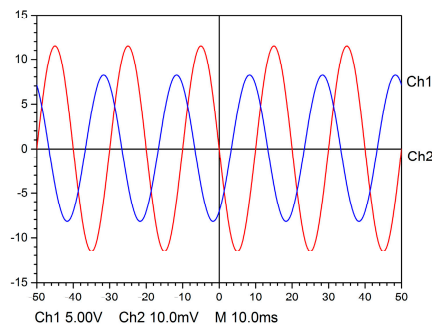


Figure 7. Experimental waveform (15 μ F, 200 turns, 3 A).

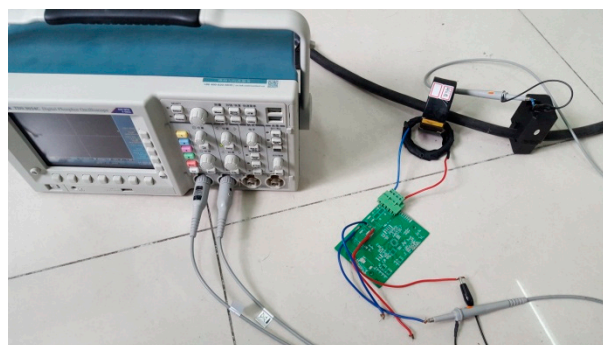


Figure 8. Test site of the experiment.

Suppose that the current generated by the power source is 3 A and the turns of the coil are 200. The output voltage peak value and φ are recorded. The positive direction is stipulated. The relation curve between the calculated output power and the load capacitance is shown in Figure 9.

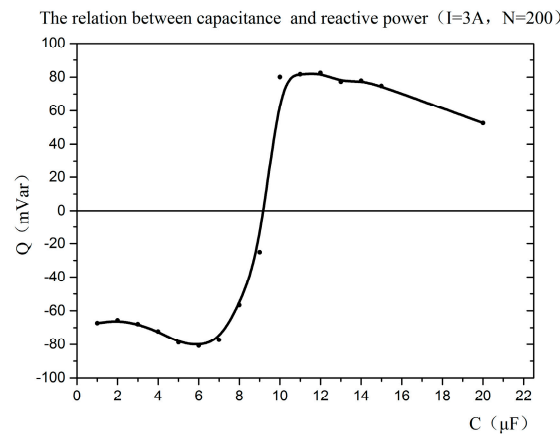


Figure 9. Relation curve between capacitance and reactive power.

Figure 9 shows that with a given fixed line current and the increase of the load capacitance, Q firstly decreases to the negative maximum, increases to positive, and then begins to decrease again after reaching the positive maximum. The device compensates the inductive reactive power to the transmission line before the zero point and compensates the capacitive reactive power after the zero point. When the system’s inductive and capacitive reactance match the internal resistance R_{Fe} , the inductive and capacitive compensating powers reach the maximum.

By substituting the experimental parameters into Equations (11), (14), and (A-10), the curve of reactive output Q , active loss P , and load capacitance C under this condition can be drawn, as shown in Figure 10. For the matching capacitance value, it can be seen through comparison that the theoretical value is basically the same as the actual value; for the power amplitude, there is a deviation between the theoretical value and the actual value, because there are multiple losses such as current transformer, experimental resistance, oscilloscope, etc., so the value is different.

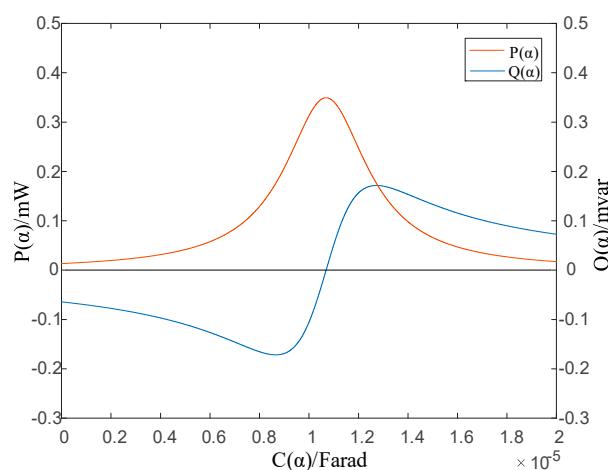


Figure 10. Relation curve between capacitance and reactive power.

3.2. Relationship between Maximum Power and Number of Turns

The relationship between the maximum output power of the coupling transformer and the number of turns was analyzed by the above experiment. The number of turns was set to 100, 200, and 300, while other experimental conditions were fixed. The relation curve is shown in Figure 11.

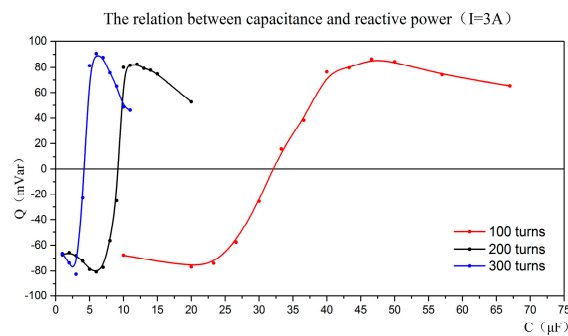


Figure 11. Relation curves between capacitance and reactive power under different numbers of turns.

It can be seen from Figure 11 that Q_{max} remains basically the same (about 90 mVar) when the number of turns changes, indicating that the Q_{max} of the coupling transformer is unrelated with the number of turns. Moreover, the capacitance corresponding to Q_{max} changes with the number of turns. The capacitance under 100 turns is 47 μF , which decreases to 12 μF under 200 turns and 6 μF under 300 turns. The capacitance is inversely proportional to the square of the number of turns.

3.3. Relationship between Maximum Power and Line Current

The relationship between the Q_{max} of the coupling transformer and the line current was studied using the magnetic core in Figure 6 and 200 turns of the coil. The currents generated by the power source were 2 and 3 A. The relation curve between Q_{max} and C was obtained by the above experiment (Figure 12).

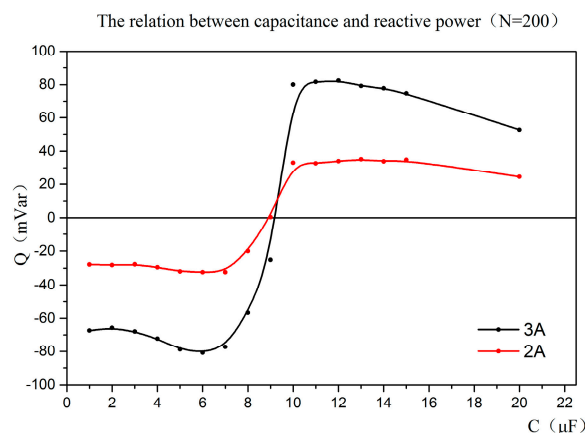


Figure 12. Relation curves between capacitance and reactive power under different line currents.

In Figure 12, Q_{max} is 35 mVar when the current is 2 A. This indicates that the reactive power is proportional to the square of the current, meeting Equations (11) and (13). The capacitance corresponding to Q_{max} remains basically the same (about 12 μF) when the current changes.

3.4. Relationship between Maximum Power and Air Gap

The relationship between the Q_{max} of the coupling transformer and the air gap thickness of the magnetic core was addressed by the experiment. The Q_{max} of the coupling transformer under different air gap thicknesses, but a fixed number of turns and line current, was measured. The air gap thicknesses in the experiment are shown in Table 2.

Table 2. Air gap thickness.

Air Gap	d1	d2	d3	d4	d5	d6
Thickness (mm)	0	0.01	0.02	0.03	0.053	0.072

The relationship between the reactive power and the load capacitance under different air gap thicknesses is shown in Figure 13.

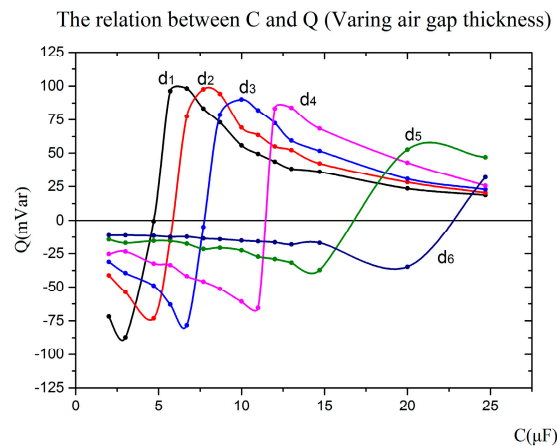


Figure 13. Relation curves between capacitance and reactive power under different air gap thicknesses.

It can be seen from Figure 13 that when the air gap increases gradually, C corresponding to Q_{max} increases, while the value of Q_{max} decreases.

In fact, the effective magnetic permeability of the whole magnetic core decreased significantly with the increase of the air gap. The magnetic core with an air gap is shown in Figure 14. The outer diameter, inner diameter, mean length of a magnetic path, air gap length, relative magnetic permeability before cutting, absolute magnetic permeability before cutting, and relative magnetic permeability after cutting of the magnetic core are marked as D_o , D_i , l_c , l_g , μ_r , μ , and μ_{rg} , respectively.

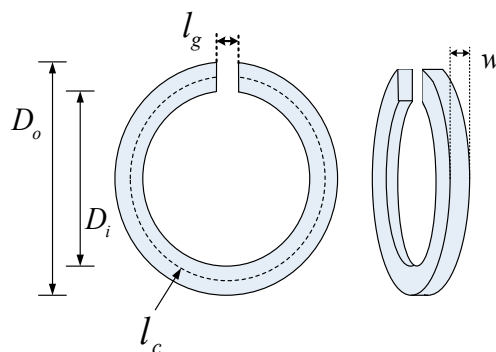


Figure 14. Magnetic core with an air gap.

According to the most common simplified magnetic core model with an air gap [20], the effective relative magnetic permeability of the magnetic core with air gap is

$$\mu_{rg} = \frac{\mu_r}{1 + \frac{l_g}{l_c + l_g} \mu_r} \tag{15}$$

Based on the simplified power output model of the coupling transformer (Figure 3) and the calculation in Appendix B, the capacitance when the magnetic core without air gap has zero reactive power is

$$C_0 = \frac{1}{2\pi f^2 N_2^2 \mu h \ln \frac{D_o}{D_i}} \quad (16)$$

Then, the absolute magnetic permeability is

$$\mu = \frac{1}{2\pi f^2 N_2^2 C h \ln \frac{D_o}{D_i}} \quad (17)$$

Substitute it into $C_0 = 4.7 \mu\text{F}$, and the relative magnetic permeability can be gained: $\mu_r = 12872$. Then, the relative magnetic permeability with the air gap was calculated according to Equation (15): 7895.4, 5694.1, 4452.8, 2965.9, and 2324.8, respectively. This revealed that the involvement of the air gap can reduce the relative magnetic permeability of the magnetic core. It can be known from Equation (11) that Q_{max} is proportional to the relative magnetic permeability (μ_r). With the increase of air gap thickness, the effective relative magnetic permeability decreases, thus reducing Q_{max} accordingly.

With the increase of air gap thickness, the power loss also declines according to Equation (11). In order to meet the output requirements, adding a thin air gap in engineering practice is necessary. It may not only reduce the power loss to some extent but also prevent the magnetic saturation of the iron core in the coupling transformer.

4. Conclusions

The power output characteristics of the coupling transformer in the D-FACTS device are discussed. The research results could provide guidance on the design of the coupling transformer, in order for the D-FACTS device to fulfil requirements pertaining to power density, heat dissipation, and design optimization.

(1) Given the fixed line current of the transmission line, the output power of the coupling transformer (Q) changed with the compensating circuit load of the secondary side. When the equivalent load capacitance (X_C) matched the magnetic inductance (X_L), $Q = 0$. When the combination of X_C and X_L matched the internal resistance (R_{Fe}), Q reached the maximum.

(2) The maximum output power of the coupling transformer (Q_{max}) was unrelated to the number of turns of the coil (N_2). The capacitance corresponding to Q_{max} was inversely proportional to the square of N_2 .

(3) Q_{max} was proportional to the square of line current (I_1), and the capacitance corresponding to Q_{max} remained unchanged.

(4) Q_{max} decreased with the increase of the air gap thickness of the magnetic core.

Author Contributions: Conceptualization and methodology, Z.H., S.Z., and Y.L.; validation and formal analysis, Z.H. and S.Z.; writing and original draft preparation, Z.H.; writing, review, and editing, Z.H., S.Z., and F.W.; funding acquisition, G.S. and X.J.

Funding: This research was funded by a grant (No. 51307109) from the National Natural Science Foundation of China and a grant (No. 13dz1201302) from the Scientific Research Plan Project of the Shanghai Science and Technology Commission.

Conflicts of Interest: The authors declare no conflict of interest.

Appendix A

The relationship between α and C is deduced by some equations in Section 2.

$$e_2 = N_2 \frac{\mu h}{2\pi} \ln \frac{D_o}{D_i} \frac{di_\mu}{dt} \quad (A1)$$

$$I_{Fe} = C_1 I_\mu^k \quad (\text{A2})$$

$$I_1 \sin \alpha = I_{Fe} \quad (\text{A3})$$

$$I_2 N_2 - I_1 \cos \alpha = I_\mu \quad (\text{A4})$$

$$E_2 = I_2 Z_L = I_2 \frac{1}{2\pi f C} \quad (\text{A5})$$

Combining Equations (A1) and (A5),

$$N_2 \mu h f \ln \frac{D_o}{D_i} I_\mu = I_2 \frac{1}{2\pi f C} \quad (\text{A6})$$

Equation (A7) could be obtained according to Equation (A6), where K_1 is a constant that includes f , N_2 , μ , h , D_o , and D_i . K_2 could be known in the same way.

$$I_2 = 2\pi f^2 N_2 \mu h \ln \frac{D_o}{D_i} I_\mu C = K_1 I_\mu C \quad (\text{A7})$$

Combining Equations (A4) and (A7),

$$I_1 \cos \alpha = I_2 N_2 - I_\mu = K_1 N_2 I_\mu C - I_\mu = K_2 I_\mu C - I_\mu \quad (\text{A8})$$

Combining Equations (A2), (A3), and (A8),

$$I_1 \sin \alpha = C_1 \left(\frac{I_1 \cos \alpha}{K_2 C - 1} \right)^k \quad (\text{A9})$$

When I_1 is determined, Equation (A9) only has two variables: α and C . Therefore,

$$C(\alpha) = \frac{1}{K_2} \left(\frac{C_1^{\frac{1}{k}} I_1 \cos \alpha}{(I_1 \sin \alpha)^{\frac{1}{k}}} + 1 \right) \quad (\text{A10})$$

In other words, there is a functional relationship between α and C .

Appendix B

When $Q = 0$, let $\cos \alpha = 0$, and the relationship between E_2 and the load is

$$E_2 = I_2 Z_L = I_2 \frac{1}{2\pi f C} \quad (\text{A11})$$

Combining Equations (A1), (A4), and (A11),

$$C_0 = \frac{1}{2\pi f^2 N_2^2 \mu h \ln \frac{D_o}{D_i}} \quad (\text{A12})$$

The magnetic inductance of the magnetic core is as follows:

$$I_\mu X_c = N_2 I_2 \frac{Z_L}{N_2^2} = \frac{E_2}{N_2} \quad (\text{A13})$$

Combining Equations (A1) and (A13), the load capacitance when $Q = 0$ is

$$C_0 = \frac{1}{N_2^2} \frac{1}{4\pi^2 f^2 L_0} \quad (\text{A14})$$

Therefore, the system output power is zero when the equivalent load capacitance matches the magnetic inductance of the magnetic core.

At Q_{max} , it can be known that

$$\frac{dQ}{d\alpha} = \mu h f \ln \frac{D_o}{D_i} C_1^{-\frac{1}{k}} I_1^{1+\frac{1}{k}} \left(\frac{1}{k} (\sin \alpha)^{\frac{1}{k}-1} \cos^2 \alpha - (\sin \alpha)^{\frac{1}{k}+1} \right) = 0 \quad (A15)$$

According to the values of k , we get that

$$\alpha_0 = \cos^{-1} \left(\frac{-k^{-1} + \sqrt{k^{-2} + 4}}{2} \right) \quad (A16)$$

or

$$\alpha_0 = 2\pi - \cos^{-1} \left(\frac{-k^{-1} + \sqrt{k^{-2} + 4}}{2} \right) \quad (A17)$$

Bringing α_0 into the power calculation formula,

$$Q = \mu h f \ln \frac{D_o}{D_i} C_1^{-\frac{1}{k}} I_1^{1+\frac{1}{k}} (\sin \alpha_0)^{\frac{1}{k}} \cos \alpha_0 \quad (A18)$$

Because α_0 has two values, Q has positive and negative maximums.

References

1. Song, Y.H.; Johns, A. *Flexible ac Transmission Systems (FACTS)*, No. 30; IET: London, UK, 1999.
2. Rogers, K.M.; Overbye, T.J. Some applications of distributed flexible AC transmission system (D-FACTS) devices in power systems. In Proceedings of the 2008 40th North American Power Symposium, Calgary, AB, Canada, 28–30 September 2008.
3. Gotham, D.J.; Heydt, G.T. Power flow control and power flow studies for systems with FACTS devices. *IEEE Trans. Power Syst.* **1998**, *13*, 60–65. [\[CrossRef\]](#)
4. Divan, D.; Brumsickle, W.; Schneider, R.; Kranz, B.; Gascoigne, R.; Bradshaw, D.; Ingram, M.; Grant, I. A distributed static series compensator system for realizing active power flow control on existing power lines. In Proceedings of the IEEE PES Power Systems Conference and Exposition, New York, NY, USA, 10–13 October 2004; pp. 654–661.
5. Divan, D.; Johal, H. Distributed FACTS-A new concept for realizing grid power flow control. In Proceedings of the 2005 IEEE 36th Power Electronics Specialists Conference, Recife, Brazil, 8–14 June 2005.
6. Jalayer, R.; Mokhtari, H. A simple three-phase model for distributed static series compensator (DSSC) in newton power flow. In Proceedings of the 2009 Asia-Pacific Power and Energy Engineering Conference, Wuhan, China, 27–31 March 2009.
7. Simfukwe, D.; Pal, B.C.; Begovic, M.; Divan, D.; Song, Y. Control of power system static stability using distributed static series compensators. In Proceedings of the 2009 IEEE Power & Energy Society General Meeting, Calgary, AB, Canada, 26–30 July 2009.
8. Johal, H. Distributed Series Reactance: A New Approach to Realize Grid Power Flow Control. Ph.D. Thesis, Georgia Institute of Technology, Atlanta, GA, USA, 2008.
9. Yuan, Z.; de Haan, S.W.; Ferreira, J.B.; Cvoric, D. A FACTS device: Distributed power-flow controller (DPFC). *IEEE Trans. Power Electron.* **2010**, *25*, 2564–2572. [\[CrossRef\]](#)
10. Li, M.; Wang, Y.; Fang, X.; Wang, Z. On high precision distributed series compensator control in static reference frame. In Proceedings of the 7th International Power Electronics and Motion Control Conference, Harbin, China, 2–5 June 2012.
11. Dorostkar-Ghamsari, M.; Fotuhi-Firuzabad, M.; Aminifar, F. Probabilistic worth assessment of distributed static series compensators. *IEEE Trans. Power Deliv.* **2011**, *26*, 1734–1743. [\[CrossRef\]](#)
12. Fajri, P.; Afsharnia, S. A PSCAD/EMTDC model for distributed static series compensator (DSSC). In Proceedings of the 2008 Second International Conference on Electrical Engineering, Lahore, Pakistan, 25–26 March 2008.

13. Rogers, K.M.; Overbye, T.J. Power flow control with distributed flexible AC transmission system (D-FACTS) devices. In Proceedings of the 41st North American Power Symposium, Starkville, MS, USA, 4–6 October 2009.
14. Yue, T.; Liu, Y.; He, Z. Power output characteristics of magnetic core in CT energy harvesting devices. *High Volt. Appar.* **2015**, *51*, 18–23.
15. Du, Y.; Liu, Y.; Shao, Q.; Luo, L.; Dai, J.; Sheng, G.; Jiang, X. Single Line-to-Ground Faulted Line Detection of Distribution Systems with Resonant Grounding Based on Feature Fusion Framework. *IEEE Trans. Power Deliv.* **2019**, *34*, 1766–1775. [[CrossRef](#)]
16. Cong, Z.; Liu, Y.; Fang, J.; Wang, P.; Guo, L.; Jiang, X. Root-Cause Identification of Single Line-to-Ground Fault in Urban Distribution Network Based on Correlation Dimension and Average Resistance. *IEEE Trans. Power Deliv.* **2019**. Early Access. [[CrossRef](#)]
17. Chapman, S.J. *Electric Machinery Fundamentals, Fourth Edition*; McGraw-Hill Inc.: New York, NY, USA, 2005.
18. Liu, Y.; Sheng, G.; Wang, K.; Lu, C.; Chen, J.; Jiang, X. A new design of current transformer energy harvesting power supply based on phase angle control method. *Autom. Electr. Power Syst.* **2011**, *35*, 72–76.
19. Liu, Y.; Xie, X.; Hu, Y.; Qian, Y.; Sheng, G.; Jiang, X.; Liu, Y. A novel high-density power energy harvesting methodology for transmission line online monitoring devices. *Rev. Sci. Instrum.* **2016**, *87*, 653–663. [[CrossRef](#)] [[PubMed](#)]
20. Flanagan, W.M. *Handbook of Transformer Design and Applications, Second Edition*; McGraw-Hill Inc.: New York, NY, USA, 1993.



© 2019 by the authors. Licensee MDPI, Basel, Switzerland. This article is an open access article distributed under the terms and conditions of the Creative Commons Attribution (CC BY) license (<http://creativecommons.org/licenses/by/4.0/>).